CFD Analysis of Heat Transfer in an Elliptic Annulus Using Nanofluids

Aman Kumar[1], Dr. Anirudh Gupta[2], Amit Singh Bisht[1], Nitin Kandpal[3], Manoj Joshi[3]
[1] PG Scholars, Department of Mechanical Engineering, BTKIT Dwarahat
[2] Associate Professor, Departmental of Mechanical Engineering, BTKIT Dwarahat
[3]PG Scholar, Departmental of Mechanical Engineering, BTKIT Dwarahat

Abstract – This work reports numerical simulation for three dimensional laminar mixed convective heat transfers at different nanofluids flow in an elliptic annulus with constant heat flux. A numerical model is carried out by solving the governing equations of continuity, momentum and energy using the finite volume method (FVM) with the assistance of SIMPLE algorithm. Four different types of nanofluids TiO_2, CuO, SiO_2 and ZrO_2, with different nanoparticles size 20, 40, 60 and 80 nm, and different volume fractions ranged from 0% to 4% using water as a base fluid were used. This investigation covers a Reynolds number in the range of 200 to 1000. The results revealed that SiO_2–Water nanofluid has the highest Nusselt number, followed by TiO_2–Water, ZrO_2–Water, CuO–Water, and lastly pure water. The Nusselt number increased as the nanoparticle volume fraction and Reynolds number increased; however, it decreased as the nanoparticle diameter increased.

Index Terms – Heat Transfer, Nanofluids, Elliptical Annulus, Volume Fraction, Nanoparticles Diameter.

1. INTRODUCTION

In an age of increasing heat fluxes and power loads in applications as diverse as power electronics, renewable energy, transportation, and medical equipment, liquid cooling systems are necessary to enhance heat dissipation, improve energy efficiency, and lengthen device lifetime. To satisfy these increasing thermal management needs, the heat transfer efficiency of conventional fluids must be improved.

Nanofluids are nanotechnology-based heat transfer fluids that are engineered by stably dispersing nanometer-sized solid particles (such as ceramics, metals, alloys, semiconductors, nanotubes, and composite particles) in conventional heat transfer fluids (such as water, ethylene glycol, oil, and mixtures) at relatively low particle volume concentrations. Nanofluids have been considered for applications as advanced heat transfer fluids for almost two decades, since they have better suspension stability compared to micron-sized solid particles, can flow smoothly without clogging the system, and provide enhanced thermal and physical properties.

Abu-Nada et al. has studied single phase Al_2O_3–water nanofluid flow in an annulus. Different viscosity and thermal conductivity models are used to evaluate heat transfer enhancement in the annulus by his work [1].

Izadi et al. have also investigated laminar forced convection of a nanofluid consisting of Al_2O_3 and water numerically in a two dimensional annulus with single phase approach. The tubes of elliptic cross section have drawn particular attention since they were found to create less resistance to the cooling fluid which results in less pumping power [2].

Velusamy and Garg have studied mixed and forced convection fluid flow in ducts with elliptic and circular cross sections. They found that irrespective of the value of the Rayleigh number, the ratio of friction factor during mixed convection to the corresponding value during forced convection is low in elliptical ducts compared to that in a circular duct as well as the ratio of Nusselt number to friction factor is higher for elliptic ducts compared to that for a circular duct. Despite the fact that these secondary flow in elliptical ducts is very small compared to the stream wise bulk flow, secondary motions play a significant role by cross-stream transferring momentum, heat and mass. On the other hand, the main advantage of using elliptic ducts than circular ducts is the increase of heat transfer coefficient [3].

Shamani et al. Numerical studies of heat transfer due to turbulent flow of nanofluids through rib–groove channel have been investigated. The continuity, momentum and energy equations are solved by the finite volume method (FVM).Four different rib–groove shapes have been examined. Four different types of nanoparticles, Al_2O_3, CuO, SiO_2, and ZnO with different volumes fractions in the range of 1–4% and different nanoparticle diameter in the range of 25–70 nm have been also studied. The computations are performed under constant temperature over a range of Reynolds number (Re) 10,000–40,000.Results indicate that the Trapezoidal with increasing height in the flow direction rib–trapezoidal groove has the best heat transfer rate and high Nusselt number. It is also found that the SiO_2 – nanofluid has the highest value of Nusselt number in comparison with the other type of nanofluids. The Nusselt number increases as the volume fraction increases and it de- creases as the nanoparticle

diameter increases. The present study shows that these Trapezoidal rib–groove using nanofluids have the potential to dramatically increase heat transfer characteristics and thus can be good candidates for the development of efficient heat exchanger device [4].

Ahmed et al. turbulent forced convection of nanofluids flow in triangular-corrugated channels is numerically investigated over Reynolds number ranges of 1000–5000.Four different types of nanofluids which are Al_2O_3, CuO,SiO_2 and ZnO–water with nano- particles diameters in the range of 30–70 nm and the range of nanoparticles volume fraction from 0% to 4% have been considered. The governing equations of mass, momentum and energy are solved using finite volume method (FVM). The low Reynolds number k–ε model of La under and Sharma is adopted as well. It is found that the average Nusselt number, pressure drop, heat transfer enhancement, thermal–hydraulic performance increase with increasing in the volume fraction of nanoparticles and with decreasing in the diameter of nanoparticles. Furthermore, the SiO_2–water nanofluid provides the highest thermal–hydraulic performance among other types of nanofluids followed by Al_2O_3, ZnO and CuO–water nanofluids. Moreover, the pure water has the lowest heat transfer enhancement as well as thermal– hydraulic performance [5].

2. MATHEMATICAL MODELING

2.1 Problem Specification

The physical model of the test section mainly consists of two concentric horizontal cylinders are used to form an annular space ranging from an elliptical tube placed at the center of a circular cylinder. The outer cylinder was made aluminium of 50.8 mm outer diameter, 1 mm thickness, and 500 mm length. The inner elliptic cylinder was made of aluminium with a major radius (r_2) of 9 mm and a length of 500 mm that had an axis ratio (r_1/r_2=1/3). Pure water, various nanoparticles and various base fluids are selected as the working fluid and the thermo physical properties assumed to be temperature independent.

Table 2.1: The thermophysical properties of different nanoparticles and different base fluids at T=300 K.

Thermo physical Properties	ZrO_2	SiO_2	TiO_2	CuO
ρ (kg/m^3)	5600	2200	4157	6500
C_p (J/kg K)	418	745	710	533
k (W/mK)	2.8	1.4	8.4	17.65

The thermo-physical properties of water and nanoparticle materials which used for simulation are shown in Table 2.1. The internal wall of the annular space (elliptic tube surface) was maintained under constant heat flux (q_h). Whereas the external wall of the annular space (circular cylinder surface) was kept isothermally at a constant Temperature (T_c).

2.2 Nanofluids Thermophysical Properties

The thermo physical properties of pure water, various nanoparticles and various base fluids which are density, heat capacity, effective dynamic viscosity, effective thermal conductivity and thermal expansion coefficient are given in Table 2.1. Meanwhile the nanofluids thermophysical properties for 20 nm particle size and volume fraction of 0–4% for various nanoparticles (TiO_2, CuO, SiO_2 and ZrO_2). These properties are calculated using the following equations:

Effective thermal conductivity:

$$k_{eff} = k_{static} + k_{brownian} \quad (2.1)$$

$$k_{static} = k_{bf}\left[\frac{(k_{np}+2k_{bf})-2\emptyset(k_{bf}+2k_{np})}{(k_{np}+2k_{bf})+\emptyset(k_{bf}+2k_{np})}\right] \quad (2.2)$$

Where k_{np} and k_{bf} are the thermal conductivity of the nanoparticle and the base fluid, respectively.

Thermal conductivity due to the Brownian motion presented by [5] as:

$$k_{brownian} = 5\times10^4\,\beta\emptyset\rho_{bf}C_{pbf}\sqrt{\frac{kT}{2\rho_{np}R_{np}}}\mathrm{f}(T,\emptyset) \quad (2.3)$$

$$f(T,\emptyset) = (0.028217\emptyset + 0.003917)\frac{T}{T_0} + (0.30669\emptyset - 0.00391123) \quad (2.4)$$

where k is the Boltzmann constant, T is the fluid temperature and T_0 is the reference temperature. The term of f (T, ϕ) is a function of temperature and particle volume fraction. The correlation of β is a function of the liquid volume that travels with a particle material expressed in Table 2 as it is given by Vijjha [5]. The effective dynamic viscosity is given as [6]:

$$\frac{\mu_{eff}}{\mu_{bf}} = \frac{1}{1-34.8\left(d_{np}/d_{bf}\right)^{-0.3}\emptyset^{1.03}} \quad (2.5)$$

where d_{bf} =[6M/Nπρ_{bf}]$^{1/3}$ μ_{eff} and μ_{bf} are the effective dynamic viscosity of nanofluid and dynamic viscosity of the base fluid, respectively, d_{np} is the nanoparticle diameter, d_{bf} is the base fluid equivalent diameter and ϕ is the nanoparticle volume fraction. M is the molecular weight of the base fluid, N is the Avogadro number =6.022_10^{23} mol^{-1} and ρ_{f0} is the mass density of the base fluid calculated at temperature T_0=293 K. The effective density is given as [6]:

$$\rho_{eff} = (1-\emptyset)\rho_{bf} \quad \emptyset\rho_s \quad (2.6)$$

Where ρ_{eff} and ρ_{bf} are the nanofluid and base fluid densities, respectively, and ρ_s is the density of nanoparticle. The effective specific heat at constant pressure of the nanofluid $(C_p)_{eff}$ is computed using the following equation [6]:

$$(C_p)_{eff} = \frac{(1-\emptyset)(\rho C_p)_{bf} + \emptyset(\rho C_p)_s}{(1-\emptyset)\rho_{bf} + \emptyset\rho_s} \qquad (2.7)$$

Where $(C_p)_s$ and $(C_p)_{bf}$ are the heat capacity of solid particles and base fluid, respectively. Properties of nanofluids at volume fraction 4% used in this study are available in Table 2.

The Reynolds number and the Nusselt number are expressed by the following relations [7]:

$$Re = \frac{\rho u_{av} D_h}{\mu} \qquad (2.8)$$

$$Nu = \frac{hD_h}{k} \qquad (2.9)$$

2.3 Boundary Conditions

At the elliptic inlet, different velocities depending on the values of Reynolds number were used, and the outlet temperature was taken as T_{in}=300 K. The constant heat flux used was 5000 W/m^2 to heat up the inside walls. At the domain outlet the flow and heat transfer are assumed to be fully developed. The boundary condition can be expressed as follows:

- At the inlet of annulus (z=0 and $r_i \le r \le r_0$) :

$$u_r = u_\theta = 0\,,$$

$u_z =$ depends on different Reynolds Number

and $T=T_{iz}$

- At the fluid wall interface ($r=r_i$ and $0 \le Z \le L$)

$$u_r = u_\theta = u_z = 0 \quad \text{and}$$

$$q_{w,i} = -k_{eff}\left[\frac{\partial t}{\partial r}\right]_{r=ri}$$

- At the outlet of annulus (z=L and $r_i \le r \le r_o$): $p=p_0$ and an overall mass balance correction is applied.

3. MODELLING AND SIMULATION

The geometry was done in the ANSYS with measurements the outer cylinder was made from aluminium of 50.8 mm outer diameter, 1 mm thickness, and 500 mm length. The inner elliptic cylinder was made of aluminium with a major radius (r_2) of 9 mm and a length of 500 mm that had an axis ratio (r_1/r_2=1/3). Pure water, various nanoparticles and various base fluids are selected as the working fluid and the thermo physical properties assumed to be temperature independent. The internal wall of the annular space (elliptic tube surface) was maintained under constant heat flux. Whereas the external wall of the annular space (circular cylinder surface) was kept isothermally at a constant temperature.

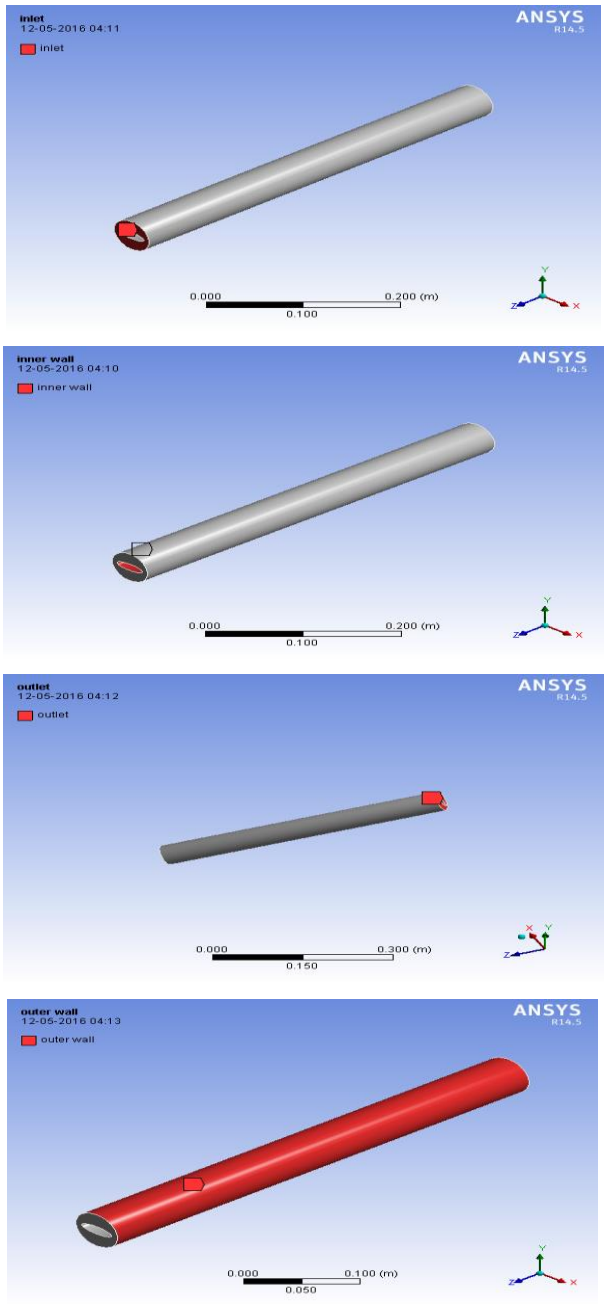

Fig 3.1: Geometry of the Elliptical Annulus

The governing equations for flow and heat transfer in the annulus are as follows [4]:

Continuity equation:

$$\frac{\partial \rho}{\partial t} + \nabla \times (\rho V) = 0 \qquad (2.1)$$

Momentum equation:

$$\rho \frac{DV}{Dt} = \nabla \times \tau_{ij} - \nabla p + \rho F \qquad (2.2)$$

Energy equation:

$$\rho \frac{De}{Dt} + \rho(\nabla \times V) = \frac{\partial Q}{\partial t} - \nabla \times q + \Phi \qquad (2.3)$$

Where V is the fluid velocity vector, F is the body forces, q represents heat transfer by conduction and Φ is the dissipation term. These governing equations along with the given boundary conditions are solved to obtain the fluid temperature distribution and pressure drop along the annulus. These data were then used to examine the thermal and flow fields along the annulus.

4. RESULTS AND DISCUSSION

4.1 The Effect of Different Types of Nanoparticles

Four different types of nanoparticles such as TiO_2, ZrO_2, SiO_2 and CuO and pure water as a base fluid are used. The nanoparticle type affects the nanofluid properties which in turn affect the heat transfer performance. The Nusselt number for different values of Reynolds number and different nanofluids are shown in Fig. 4.1. It can be obviously seen that SiO_2 nanofluid has the highest surface Nusselt number, followed by TiO_2, ZrO_2, and CuO respectively. This is because SiO_2 has the lowest thermal conductivity than other nanofluids, but higher than water and has the highest average velocity among other fluids due to its lowest density compared with the others. The surface Nusselt number increases significantly as Reynolds number increases for the four nanofluids types. It is less dense and this property enables the particle to move rapidly in the annulus tube and it characterizes the main reason to give high heat transfer coefficient. In general, the value of Nusselt number is inversely proportional to the value of thermal conductivity of that particular fluid.

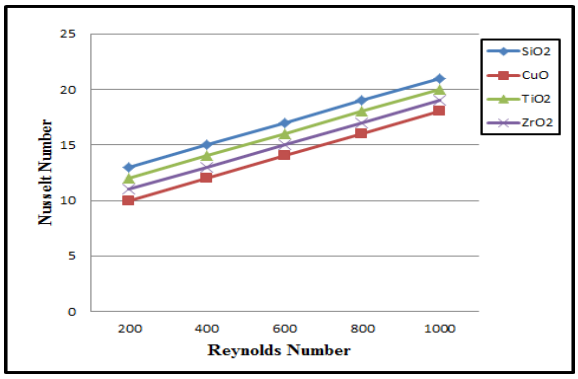

Fig.4.1: Effect of different nanofluids types at different Reynolds numbers for Nusselt number

4.2 The Effects of Nanoparticles Volume Fraction

The effect of nanoparticles volume fraction on the average Nusselt number with different Reynolds number at dp=20 nm is depicted in Fig 4.2. At a given Reynolds number, it can clearly see that the average Nusselt number increases as the volume fraction of the nanoparticles increases due to improve the thermal conductivity of the nanofluid. It can also be seen at particular volume fraction; the average Nusselt number increases with increasing Reynolds number due to increases the temperature gradient at the wall. This is because as the volume fraction increases, irregular and random movements of the particles increases the energy exchange rates in the fluid with a penalty on the wall shear stress and consequently augment the thermal dispersion of the flow.

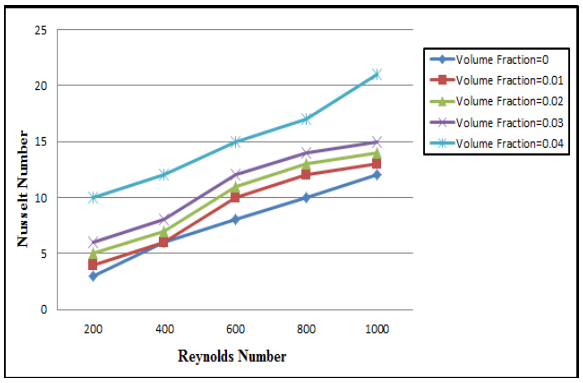

Fig.4.2: Different volume fraction at different Reynolds numbers for Nusselt number

4.3 Effect of Different Nanoparticle Diameter

Fig.4.3 shows the effect of the nanoparticles diameter on the average Nusselt number with different Reynolds numbers at 4% volume fraction of the SiO_2–water nanofluid. According to this figure, it is found that the average Nusselt number increases as the particle diameter decreases. This is because the surface area per unit volume increases with decreasing in the particle diameter. In addition, the Brownian motion is higher for the smaller particles.

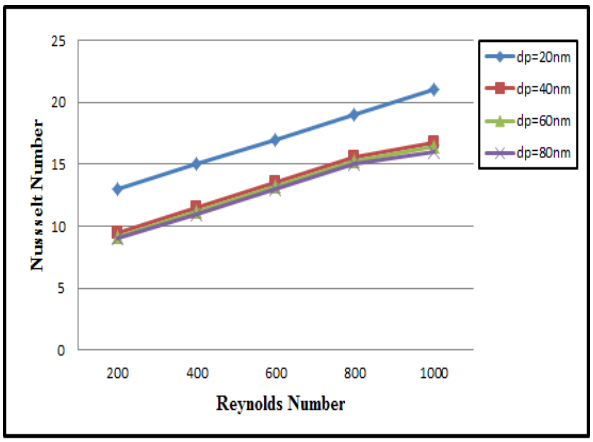

Fig.4.3: Different nanoparticles diameters at different Reynolds number for Nusselt number.

5. CONCLUSIONS

Numerical simulations of laminar mixed convection heat transfer using nanofluids such as TiO_2, CuO, SiO_2 and ZrO_2 as the working fluids in an elliptic annulus with uniform heat flux were reported. The emphasis is given on the heat transfer enhancement resulting from various parameters, which include nanofluid types, volume fraction of nanoparticle, nanoparticle diameter and base fluid type. The governing equations were solved utilizing finite volume method with certain assumptions and appropriate boundary conditions.

The results were obtained through the numerical simulation that gives the highest Nusselt number. It is clearly observed that the best setting of parameters that gave the best heat transfer enhancement through the elliptic annulus were by using SiO_2 (silicon dioxide) as the working fluid with percentage of concentration of 4%, diameter of particle (dp) of 20 nm.

The Nusselt number is remarkably increased with the increase of nanoparticle volume fraction and Reynolds number; however, it is decreased with the increase of nanoparticles diameter.

REFERENCES

[1] Abu-Nada E. Effects of variable viscosity and thermal conductivity of Al_2O_3–water nanofluid on heat transfer enhancement in natural convection. International Journal Heat Fluid Flow 2009;30(4):679–90.
[2] Izadi M, Behzadmehr A, Jalali-Vahida D. Numerical study of developing laminar forced convection of a nanofluid in an annulus. International Journal Thermal Science.2009;48:2119–29.
[3] Velusamy K, Garg VK. Laminar mixed convection in vertical elliptic ducts International Journal Heat Mass Transfer 1996;39(4):745–52.
[4] Shamani A.N.,Sopian K.,Mohammed H.A. Enhancement heat transfer characteristics in the channel with Trapezoidal rib–groove using nanofluids. Case Studies in Thermal Engineering 5 (2015)48–58
[5] Ahmed M.A., Yusoff M.Z. , Ng K.C., Numerical investigations on the turbulent forced convection of nanofluids flow in a triangular-corrugated channel. Case Studies in Thermal Engineering 6 (2015)212–225
[6] Vijjha RS, Das DK. Experimental determination of thermal conductivity of three nanofluids and development of new correlations. International Journal of Heat Mass Transfer 2009;52:4675–82.
[7] Corcione M. Heat transfer features of buoyancy-driven nanofluids inside rectangular enclosures differentially heated at the sidewalls. International Journal Thermal Science 2010;49:1536–46.
[8] Velusamy K, Garg VK, Vailyanathan G. Fully developed flow and heat transfer in semi-elliptical ducts. . International Journal Heat Fluid Flow 1995;16:145–52.
[9] Sakalis VD, Hatzikonstaninoi PM, kafousias N. Thermally developing flow in elliptic ducts with axially variable wall temperature distribution International Journal Heat Mass Transfer 2002;45:25–35.
[10] Eiamsa-ard S, Promvonge P. Thermal characteristics of turbulent rib-grooved channel flows. International Communication Heat Mass Transfer 2009; 36:705–11.